ELSEVIER

Catalysis Today 70 (2001) 369–382

CATALYSIS TODAY

www.elsevier.com/locate/cattod

Pattern formation in models of fixed-bed reactors

Moshe Sheintuch*, Olga Nekhamkina

Wolfson Department of Chemical Engineering, Technion, Israel Institute of Technology, Haifa 32000, Israel

Abstract

This work reviews and compares spatiotemporal patterns in three models of adiabatic fixed catalytic beds for reactions with oscillatory kinetics: homogeneous and heterogeneous models, which are studied using generic first-order kinetics, and a detailed model of CO oxidation in the monolithic reactor. These three models describe reactors with one, two or all three phases (fluid-, solid- and adsorbed-phases), respectively. Pattern selection is based on the oscillatory or bistable nature of the kinetics and on the nature of fronts. The heterogenous and detailed models may exhibit local bistability while the homogeneous model does not admit this property: a simple conversion between the parameters of the homogeneous and heterogeneous models is suggested.

The spatiotemporal patterns in the reactor can be predicted from the sequence of phase planes spanned by the reactor. Stationary or oscillatory front solutions, oscillatory states that sweep the whole surface or excitation fronts may be realized in the homogeneous and heterogeneous models. The detailed model of the converter may exhibit oscillatory motion, which may be periodic or chaotic, in which typically a hot domain enters the reactor exit and moves quickly upstream; the following extinction occurs almost simultaneously due to strong coupling by convection.

Keywords: Fixed-bed reactors; Spatiotemporal patterns; Heterogeneous model; Homogeneous model

1. Introduction

While the interaction of diffusion and nonlinear kinetics has been extensively investigated, the study of patterns in reaction–convection–conduction systems is only now emerging. The experimental identification of patterns observed in heterogeneous reactors is still ambiguous in many cases, partly due to experimental difficulties and nonuniformity of the system properties. Spatial structures simulated in heterogeneous reactors differ from those known to exist in reaction–diffusion systems due to convective effects. The existence of such patterns is a practical problem which should affect design and operation procedures of commercial reactors like the catalytic converter: oscillatory behavior has been observed during the oxidation of carbon-monoxide, hydrogen, ammonia, hydrocarbons, alcohols, ethers and formic acid, as well as during nitrogen-monoxide reduction by ammonia or carbon-monoxide and the hydrogenation of carbon-monoxide or ethylene. Most of these reactions are of commercial importance in pollution-abatement and other processes.

This work reviews a hierarchy of fixed-bed mathematical models along with the corresponding class of spatiotemporal patterns that may emerge in high-pressure catalytic fixed-bed reactors. In high-pressure reactors thermal effects provide the positive-feedback as well as the long-range communication and thermal patterns usually emerge due to the interaction of the catalyst with flow. Thus, we study nonisothermal models of such reactors. Our

* Corresponding author. Tel.: +972-4-829-2823; fax: +972-4-8230-476.
E-mail address: cermsll@techunix.technion.ac.il (M. Sheintuch).

0920-5861/01/$ – see front matter
PII: S0920-5861(01)00344-3

Nomenclature

A	preexponential factor
A_v	interphase surface area per catalyst volume
B	dimensionless exothermicity
C_A, C_{Af}	key component concentration in solid and fluid-phase, respectively
D_a	Damkohler No.
D_e	effective axial dispersion coefficient
E	activation energy
f, g	kinetic functions
h	interphase heat transfer coefficient
ΔH	reaction enthalpy
k_{d+}, k_{d-}	activation and deactivation rate constants, respectively
k_e	effective axial conductivity
k_g	mass transfer coefficient
k_i	rate constants for CO and oxygen adsorption (1, 2) and desorption (-1, -2), and their reaction (3)
K	deactivation parameter
L	reactor length
L_T	conduction length scale
Le	Lewis No.; the ratio of solid to fluid-phase heat capacities
M	deactivation parameter
Pe_T, Pe_C	Peclet numbers for heat- and mass-dispersion
r, r_{ref}	reaction rate and its characteristic value
t	time
T, T_f	solid and fluid temperature, respectively
u_s	interstitial fluid velocity
V	front velocity
x, y, X, Y	dimensionless solid- and fluid-phase concentration and temperature
z	dimensional and dimensionless axial coordinate

Greek symbols

α_i	stoichiometric co-efficient
β_C, β_T	dimensionless interphase transport coefficient
γ	dimensionless activation energy
ε	bed void fraction
θ	adsorbed-phase concentrations
θ^*	activity
ρc_{pf}, $\rho_s c_{ps}$	volumetric specific heat capacity of the fluid- and solid-phases, respectively
τ	dimensionless time
τ_T	solid-phase thermal time scale

Subscripts

C, T, θ	respective variables
i	species i
in	value at the inlet
s	at steady state

current understanding of catalytic oscillators suggests that they are governed by the interaction of a fast and long-range autocatalytic-variable (typically, the temperature) with a slow and localized changes in catalytic activity. Such one-dimensional systems are excitable but are unlikely to exhibit sustained spatiotemporal patterns in the absence of global-interaction or flow. This review focuses, therefore, on the interaction of the fluid-phase, through which the reactants are supplied, and the reactive solid-phase. This interaction may produce patterns under conditions that in the absence of such interaction induce homogeneity in the catalyst phase. Experimentalists had tried to minimize this interaction by increasing the fluid flow-rate into the reactor, or by applying control to the gas-phase concentration.

We describe below three fixed-bed reactor models, differing in the number of phases they account for: In the *homogeneous model*, gradients between the solid and fluid-phases are neglected and the rates are expressed in terms of the fluid-phase concentration and temperature [16]. The *heterogeneous model* accounts for both phases, and for heat and mass exchange between them, and the rates are expressed in terms of the solid-phase temperature and pore-phase concentration. In both models we employ a generic first-order exothermic kinetics [2,17]. *A detailed model* accounts for both phases as well as for an adsorbed-phase, and the rate is expressed in terms of fractional surface coverage and solid temperature. Keren and Sheintuch

[9] employed, after some modification, the Sales et al. [13] oscillatory kinetics model for CO oxidation on Pt to study pattern formation during Pt-catalyzed CO oxidation in the monolithic reactor. All models are analyzed for realistic conditions, of high heat capacity and low thermal conductivity (high *Pe*), and employ a slow process of changes in activity to induce the oscillations. Inspection of the time and length scales associated with the various variables show that all models can be described by a fast and diffusive activator (temperature) and a slow localized inhibitor (activity), and that their mode of interaction is quite similar and consequently they predict similar patterns. We do not elaborate on the detailed kinetics of bistable or oscillatory catalytic reactions: several reviews of catalytic oscillatory kinetics under high-pressure [14,22] as well as under low-pressures [4] are available.

Pattern formation can be qualitatively understood in terms of front motion and analysis of the sequence of phase planes spanned by the reactor. Heterogeneous reactors are characterized by an hierarchical structure: a catalytic site, a crystallite, a pore, a pellet and a reactor. Each of these levels of organizations may be assumed to be spatially homogeneous while patterns appear only on a larger scale. Communication on a large scale is poorer as certain species cannot diffuse: adsorbates may diffuse and transmit information only on a continuous surface, gas-phase species diffuse only in the pore or pellet and interpellet communication is limited to heat conduction. The dependence of the global dynamic behavior on the nature of the local dynamics (i.e., phase plane) repeats itself on various scales. In the homogeneous model we employ only the reactor level. In the heterogeneous model the catalyst phase (pellet, washcoat) can exhibit oscillations or fronts for fixed fluid conditions. The question that we want to address then is what patterns are possible when convection is accounted for? In a detailed model the adsorbed-phase can exhibit this behavior for fixed temperature and concentration. What motions are possible then on the pellet and reactor levels?

The scope and structure of the review are as follows: In Section 2 we draw a schematic general model and several condensed models that were analyzed in detail. A qualitative analysis is conducted in Section 3 and simulated patterns are presented in Section 4. Some experimental results are reviewed in Section 5 along with suggestions for future experimental work aimed to reveal new patterns.

2. Reactor models

We write now a general model of a one-dimensional catalytic reactor and divide its description into three phases: the fluid-, the solid- and the adsorbed-phase. Within each phase we present several simple asymptotes and condense the information into a simple qualitative model that captures most of the features of the original model.

2.1. The fluid-phase

The general fluid-phase balance is a conventional model of a reactor with heat and mass transfer resistance, and the balances typically account for accumulation, convection, and transport to the solid-phase; axial dispersion is neglected here and heat loss by a coolant is ignored as we limit the study to adiabatic reactors. Using conventional notation the model can be written as

$$\varepsilon\frac{\partial C_{\mathrm{f}i}}{\partial t}+u_{\mathrm{s}}\frac{\partial C_{\mathrm{f}i}}{\partial z}=-k_{\mathrm{g}i}A_v(C_{\mathrm{f}i}-C_i) \tag{1}$$

$$\varepsilon\rho c_{\mathrm{pf}}\frac{\partial T_{\mathrm{f}}}{\partial t}+u_{\mathrm{s}}\rho c_{\mathrm{pf}}\frac{\partial T_{\mathrm{f}}}{\partial z}=-hA_v(T_{\mathrm{f}}-T) \tag{2}$$

where T is the solid-phase temperature and C_i the concentration within the pores or the boundary layer of the catalyst phase, T_{f} and $C_{\mathrm{f}i}$ are the corresponding fluid-phase variables.

2.2. The solid-phase

The solid-phase enthalpy balance accounts for accumulation, conduction, heat generation by reaction and heat loss to the fluid while the mass-balance accounts for similar terms but diffusion is ignored:

$$\begin{aligned}(1-\varepsilon)\rho_{\mathrm{s}}c_{\mathrm{ps}}\frac{\partial T}{\partial t}-k_{\mathrm{s}}(1-\varepsilon)\frac{\partial^2 T}{\partial z^2}\\ =(-\Delta H)(1-\varepsilon)r(C_i,T,\theta_i,\theta^*)+hA_v(T_{\mathrm{f}}-T),\\ (1-\varepsilon)\frac{\partial C_i}{\partial t}=-\alpha_i r(C_i,T,\theta_i,\theta^*)+k_{\mathrm{g}i}A_v(C_{\mathrm{f}i}-C_i)\end{aligned} \tag{3}$$

θ^* is the fraction of active sites. Typically, the mass-balance is established much faster than the enthalpy balance, while the diffusion length is smaller than the conduction length. Thus, if the solution to the mass-balance is single-valued, it may be substituted into the enthalpy balance equation (3), with fixed fluid conditions, are typical reaction–diffusion equation that can sustain front motion when they admit bistability or pulse motion when coupled with a slow variable. The enthalpy balance can be written as a reaction–diffusion problem

$$\tau_T \frac{\partial T}{\partial t} - L_T^2 \frac{\partial^2 T}{\partial z^2} = \frac{(-\Delta H) r(C_i, T, \theta_i, \theta^*)}{h A_v} - (T - T_f) \tag{4}$$

The temporal scale of thermal relaxation, $\tau_T = (\rho c_p)_s / h A_v$, is typically 1 s, in order of magnitude, and is much smaller than the characteristic time scale of the activation or deactivation processes. The characteristic thermal diffusion length in the solid-phase, $L_T = (k_s / h A_v)^{0.5}$, is much smaller than the reactor length.

2.3. The adsorbed-phase

Here we must resort to a particular reaction: a detailed kinetic model for CO oxidation on Pt or Pd (e.g. [13]) incorporates CO adsorption, oxygen dissociative adsorption and a Langmuir–Hinshelwood (LH) reaction between adsorbed CO and O atoms, which has been well established as the dominant mechanism for this reaction over a wide range of reaction parameters:

$$\mathrm{CO} + [^*] \underset{k_{-1}}{\overset{k_1}{\leftrightarrow}} [\mathrm{CO}^*] \tag{5a}$$

$$\mathrm{O_2} + 2[^*] \underset{k_{-2}}{\overset{k_2}{\leftrightarrow}} 2[\mathrm{O}^*] \tag{5b}$$

$$[\mathrm{O}^*] + [\mathrm{CO}^*] \overset{k_r}{\rightarrow} \mathrm{CO_2} + 2[^*] \tag{6}$$

[*] denotes a free adsorption site on the metal surface. The system of differential equations describing the dynamic behavior is [13]

$$\frac{\mathrm{d}\theta_1}{\mathrm{d}t} = k_1 P_{\mathrm{CO}} (1 - \theta_1 - \theta_2 - \theta^*) - k_{-1}\theta_1 - k_3 \theta_1 \theta_2 - [k_4 \theta_1 \theta^*] = f_1(T, C, \theta, \theta^*) \tag{7a}$$

$$\frac{\mathrm{d}\theta_2}{\mathrm{d}t} = k_2 P_{02} (1 - \theta_1 - \theta_2 - \theta^*)^2 - k_{-2}\theta_2^2 - k_3 \theta_1 \theta_2 - [k_5 \theta_2 (1 - \theta^*)] = f_3(T, C, \theta, \theta^*) \tag{7b}$$

where the terms in square brackets appear due to slow changes in activity (see below). Again, these balances are of importance only when $f_i(T, C, \theta, \theta^*) = 0$ is multivalued within a certain domain of parameters; otherwise they can be solved and substituted into the rate.

2.4. Catalyst activity

The nature of the slow variable (θ^*), in general, has to be specified for each oscillator. Various forms of a buffer step were incorporated to account for oscillations at high pressures. A step of the form of a slow oxidation and reduction by CO of the metal surface layer was first suggested by Sheintuch and Schmitz [18] and by Sales, Turner and Maple (STM) [23] and has received most of the experimental support as the explanation of the slow step during oscillations under atmospheric conditions. Oxide formation during this reaction was inferred from the in situ IR study by Lindstrom and Tsotsis [11] and from solid electrolyte potentiometry experiments [24]. Hartmann et al. [6] using in situ X-ray, showed that silica-supported Pt-clusters catalyzing CO oxidation underwent reversible oxidation to $\mathrm{PtO/Pt_3O_4}$. The rates of oxidation and reduction of the catalyst are orders of magnitude lower than the rates of surface reactions (typically, $\mathrm{s^{-1}}$); this explains the long oscillation periods and the wide separation between the time scales of reaction and changes in activity. Nonnoble metals can undergo bulk oxidation and reduction and for such systems changes in activity were attributed to changing oxidation states of the catalyst: Kurtanjek et al. [10] measured periodic variation of the work function during hydrogen oxidation on Ni catalyst. The mechanism of surface reconstruction, which is well established for oscillations on single crystals under low-pressure conditions (Imbihl and Ertl, 1995, [8]) was ruled out. The smaller clusters are oxidized more readily.

In all the mechanisms presented above, the inhibitor — the fraction of the active surface area (θ^*) — is

nondiffusing and the general form of its balance is

$$\frac{d\theta^*}{dt} = g(T, C, \theta_i, \theta^*) \tag{8}$$

In our study of generic first-order kinetics we adopted a simple linear expression for $g(T, \theta)$, that assumes that deactivation occurs faster at higher temperatures and at higher activities and that it is independent of reactant concentration so that it can be expressed by a single line in the (T, θ) phase plane: $g(T, C, \theta_i, \theta^*) = -[k_{d-} + \mu(T - T_{in})]\theta^* + [k_{d+} - \mu(T - T_{in})](1 - \theta^*)$ (see [2] for justification).

In the detailed model we use the expression suggested in [13]

$$\frac{d\theta^*}{dt} = k_4\theta_1\theta^* - k_5\theta_2(1-\theta^*) = g(T, C, \theta_{\tau i}, \theta^*) = 0 \tag{9}$$

2.5. Condensed models

2.5.1. The homogeneous model

If we assume that gradients of temperature and concentrations between the phases can be ignored, we can combine the equations for the two phases. In case of a first-order activated kinetics, $r = \theta^* A\, e^{-E/RT} C_A$, the model, written in terms of conventional notation of dimensionless parameters and variables, reduces to

$$\begin{aligned}
&\frac{\partial x}{\partial \tau} + \frac{\partial x}{\partial \xi} - \frac{1}{Pe_C}\frac{\partial^2 x}{\partial \xi^2} \\
&\quad = Da\,\theta^*(1-x)\exp\left(\frac{\gamma y}{\gamma + y}\right) = f_1(x, y, \theta^*), \\
&Le\frac{\partial y}{\partial \tau} + \frac{\partial y}{\partial \xi} - \frac{1}{Pe_T}\frac{\partial^2 y}{\partial \xi^2} \\
&\quad = B\,Da\,\theta^*(1-x)\exp\left(\frac{\gamma y}{\gamma + y}\right) = f_2(x, y, \theta^*), \\
&\xi = 0,\ \frac{\partial x}{\partial \xi} = Pe_C x,\ \frac{\partial y}{\partial \xi} = Pe_T y; \\
&\xi = 1,\ \frac{\partial x}{\partial \xi} = \frac{\partial y}{\partial \xi} = 0
\end{aligned} \tag{10}$$

with x (conversion) and y (dimensionless temperature) as its fast dynamic variables; see [16] for the definition of other parameters.

The multiplicity and dynamics (with $Le = 1$ and $\theta^* = 1$) of the homogeneous axial dispersion reactor has been a subject of extensive investigation in 1970 and 1980s. Steady-state multiplicity is predicted by the axial-dispersion model with sufficiently large ratio of axial diffusion to convection terms (i.e., small $Pe^{(-1)} = D_e/a_{SL}$). The homogeneous model was reviewed by Hlavacek and Van Rompay [7]. This model cannot account for observations of catalytic oscillations due to the high heat capacity and since instabilities have been observed on a single-crystal, pellet or wire even in the absence of interaction with the gas-phase. Furthermore, for reasonable values of parameters the axial-dispersion model predicts oscillations that are much faster than those observed experimentally.

The heterogeneous model for the same first-order kinetics takes the form

$$\begin{aligned}
&(1-\varepsilon)\frac{\partial x}{\partial \tau} = Da\,\theta^*(1-x)\exp\left(\frac{\gamma y}{\gamma + y}\right) - \beta_C(x - X) \\
&\qquad = f_1(x, y, \theta^*), \\
&(Le - \varepsilon)\frac{\partial y}{\partial \tau} - \frac{1}{Pe_T}\frac{\partial^2 y}{\partial \xi^2} \\
&\quad = B\,Da\,\theta^*(1-x)\exp\left(\frac{\gamma y}{\gamma + y}\right) - \beta_T(y - Y) \\
&\quad = f_2(x, y, \theta^*)
\end{aligned} \tag{11}$$

for the solid-phase, where x and y are the solid-phase conversion and temperature, respectively, and

$$\begin{aligned}
&\varepsilon\frac{\partial X}{\partial \tau} + \frac{\partial X}{\partial \xi} = \beta_C(x - X), \\
&\varepsilon\frac{\partial Y}{\partial \tau} + \frac{\partial Y}{\partial \xi} = \beta_T(y - Y)
\end{aligned} \tag{12}$$

for the fluid-phase, where X and Y are the fluid-phase variables.

The slow process in both cases is described by

$$\begin{aligned}
&\tau_\theta\frac{\partial \theta^*}{\partial \tau} = -\frac{M}{\gamma}y - (1 + K)\theta^* + K \equiv g(y, \theta^*), \\
&\tau_\theta = \frac{u_s}{Lk_{d-}},\ K = \frac{k_{d+}}{k_{d-}},\ M = \frac{\mu T_{in}}{k_{d-}}
\end{aligned} \tag{13}$$

We tested several forms of the boundary conditions: (a) the common form, with $X = Y = 0$ at $\xi = 0$ and no-flux conditions for the solid-phase, $y_\xi = 0$ at $\xi = 0, 1$; (b) conditions that account for the existence of finite-length inert zones on both sides of the catalytic bed; (c) analytical conditions that reflect

the existence of such long inert zones (see detailed discussion in [10]).

2.5.2. The transformation

Of the various analogies between the two models we tested the suggestion by Vortmeyer and Schaefer [25] that the solution of a heterogenous model can be approximated by using an effective conductivity (i.e., *Pe*) in the pseudo-homogeneous model that should be corrected as

$$\frac{1}{Pe_{T,\mathrm{hom}}} = \frac{1}{Pe_{T,\mathrm{het}}} + \frac{1}{\beta_T} \tag{14}$$

We test this condition below and show that it is a good approximation when $\beta_T \gg Pe_T$ but fails under other conditions. The criterion for the equivalence of the mass-balance of one- and two-phase models may be derived, following [25], to be, in the general case,

$$\frac{1}{Pe_{C,\mathrm{hom}}} = \frac{1}{Pe_{C,\mathrm{het}}} + \frac{1}{\beta_C} \tag{15}$$

Since we assumed $Pe_C \to \infty$ in the heterogeneous model (Eq. (3)) we use $Pe_C = \beta_C$ in all simulations with the homogeneous model below.

The *detailed model* for CO oxidation in air on Pt is not reproduced here (see [9]); it accounts for plug-flow fluid-phase balances for both species as well as for temperature, for the solid-phase balances (Eq. (3)) while ignoring mass dispersion and for the detailed models of the adsorbed-phase (Eqs. (7a) and (7b)). The rate is proportional to the LH step, with $r \sim k_3\theta_1\theta_2$. The catalyst activity follows Eq. (9). The parameters are typical for the automotive monolithic converter.

3. Qualitative analysis

Patterns selection in a simple reaction–diffusion system, in the absence of convection, is determined by the phase plane of the system and its ability to admit front solutions. Pattern selection in a bed, where convection is accounted for, will be shown to be dominated by the nature of interaction of the catalytic and fluid-phases and by the sequence of phase planes spanned by the reactor as we vary the gas-phase conditions: the solid-phase model in the heterogeneous or detailed models (Eq. (4)) describes a one-dimensional reaction–diffusion system, like a catalytic wire or a washcoat on the reactor wall, exposed to uniform gas-phase conditions (constant T_f, C_{fi}). Fronts may be induced within a domain of the reactor where the solid-phase admits multiple solutions. In the absence of convection, the system may be excited to form traveling fronts or pulses but they propagate out of the system, which eventually attains a uniform state. The interaction with convection in the fluid-phase introduces new motions and patterns. Homogeneous models do not admit local bistability but they may sustain front motion: creeping reaction zones, first reported by Frank-Kamenetskij [5] and Wicke and Vortmeyer [26], are encountered typically in response to a step-change in operating conditions.

We define the interaction between the solid- and fluid-phases to be *symmetry-breaking* (*symmetry-preserving*) if local ignition or extinction at one spot on the catalyst inhibits (accelerates) the same process in another one. In an adiabatic bed the convection

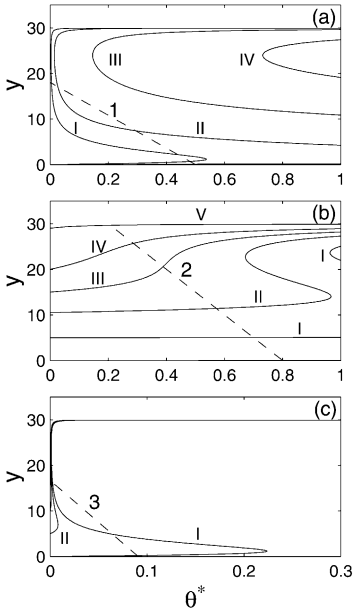

Fig. 1. Typical phase planes in a heterogeneous reactor, showing the enthalpy nullcurves (Eq. (16), solid lines) and the activity nullcurves (broken lines): (a) $Da = 0.5$, $Y = 0$, and various β_T: 20 (I), 100 (II), 1000 (III), 5000 (IV); $K = 1$, $M = 1.11$ (line 1); (b) $Da = 0.06$, $\beta_T = 1000$, and various Y: 5 (I), 10.5 (II), 15 (III), 20 (IV), 29 (V); $K = 4$, $M = 2$ (line 2); (c) $Da = 0.06$, $\beta_T = 1$, and various Y: 0 (I), 5 (II); $K = 0.1$, $M = 0.12$ (line 3) (after [17]).

will tend to synchronize transitions in the reactor, since ignition at the inlet will raise the fluid temperature and induce a similar event downstream. This will be especially true with reactions of negative-order kinetics (e.g. CO oxidation on Pt), since ignition upstream will deplete reactants downstream and induce ignition. In an isothermal bed, in which an oscillatory A + B → P reaction occurs, the interaction is symmetry-preserving when the limiting reactant is rate-inhibiting while when a rate-accelerating reactant is limiting the system tends to break the symmetry (see analysis by Shvartsman and Sheintuch [21]).

3.1. Phase plane analysis

To present the local phase planes we lump the fast-variables, those of the solid and adsorbed-phases, into the fast nullcurve ($F = 0$) while the surface modification ($g = 0$, Eq. (9)) is the slowest one. We plot a family of curves for fixed fluid concentration and temperature. Here we need to distinguish between models that admit local bistability of $F = 0$ and those that do not, like the homogeneous models.

In the case of the heterogeneous model we present the nullcurves in the (y, θ^*) plane with Y or β_T as a parameter. We assume that the surface mass-balance is in pseudo-steady-state and that the fronts are extremely slow and consequently the adiabatic relation between the enthalpy and mass balances is retained, $Y = BX$. The local fast nullcurve is described then by

$$B\beta_C f'(y, \theta^*, X) - \beta_T (y - Y) \equiv F(y; \theta^*, X, Y) = 0,$$
$$f' = (1 - X)\left[\beta_C \frac{\exp(-y/(1 + y/\gamma))}{Da\,\theta^*} + 1\right]^{-1} \quad (16)$$

$F(y, \theta^*) = 0$ is typically S-shaped while $g(y, \theta^*) = 0$ is monotonic (Fig. 1). The steady state of the local problem, the intersection of the $F(y, \theta^*) = 0$ and $g(y, \theta^*) = 0$, is stable when located on the upper or lower branches of $F(y, \theta^*) = 0$ and unstable when located on the intermediate branch and when time-scale separation is sufficiently wide. The steady state is usually classified as *excitable*, when a stable steady state

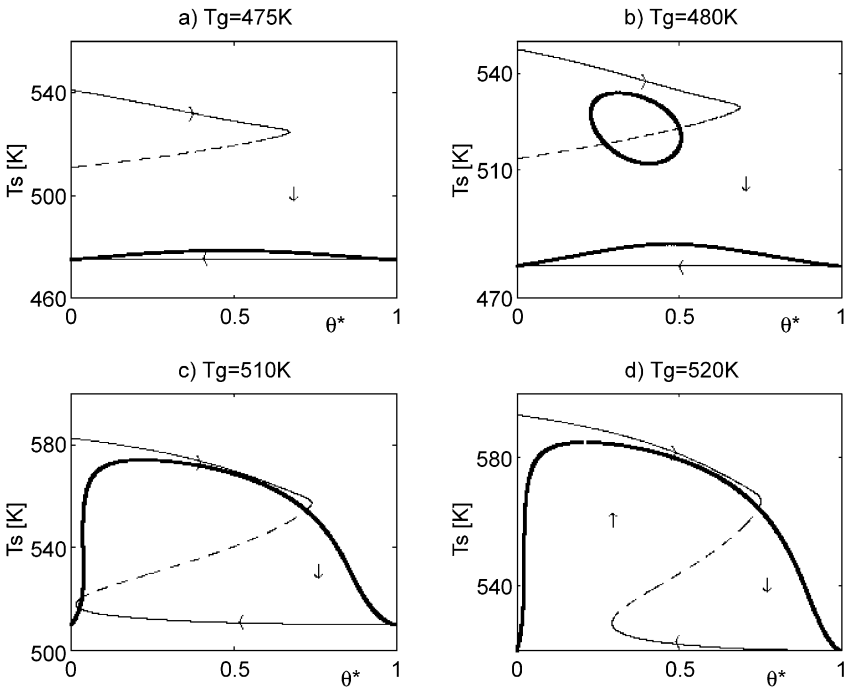

Fig. 2. Phase planes of the catalyst particle (lumped system) at different gas temperatures. $P_{CO} = 0.01$, $P_{O_2} = 0.21$; (—) stable $F(T, \theta)$ branch, (- - -) unstable $F(T, \theta)$ branch, (▬) $G(T, \theta)$ (after Keren and Sheintuch).

is located near the limit points of $F(y, \theta^*) = 0$, as *oscillatory*, when the steady state is unstable and unique, and as *bistable* when two stable states are possible. We may also find a situation with one stable and two unstable states (a saddle and a node, Fig. 1a, line 1): Fig. 1b presents a family of such curves showing the transition from an extinguished state to an ignited one, through a bistable phase plane.

Obviously the homogeneous model cannot account for bistable nullcurves (Eq. (16) with $\beta_C = \beta_T = \infty$). When *flow terms* are accounted for in the homogeneous model, however, then bistable nullcurves may be admitted for sufficiently small *Pe*. The reactor model are typically solved using a finite-difference approximation. A meaningful approximation will use cells that are of the front-width in size. Let us choose cells of size $2/Pe_T$ for which the homogeneous and heterogeneous models can be shown to be equivalent as $Da \to 0$ (see references in [1]): with $\beta_C = \beta_T = \frac{1}{2}Pe_T$ the corresponding nullcurves in the phase plane are described by Eq. (16) with y_{i-1} (the temperature at cell $(i-1)$) as a parameter (instead of *Y*). Bistability may be realized within a range of Pe_T (see [16] for a detailed analysis).

Fig. 1 presents several cases of phase plane sequence that will be used below. Fig. 1a demonstrates the effect of β_T (with equal β_C) on the phase plane in the absence of convection. These can be used to approximately characterize the effect of convection in either a homogeneous model (use effective $\beta_T = \frac{1}{2}Pe_T$) or in a heterogenous model (use effective $\beta_T = ((1/\beta_T) + (2/Pe_{T,\text{het}}))^{-1}$).

3.1.1. Boundary conditions

The behavior of the heterogeneous reactor is sensitive to the boundary conditions imposed, and these should match closely the actual physical situation [17]. Comparison of the temporal behavior of the solid- and fluid-temperatures, for the three kinds of boundary conditions, show that the no-flux condition yields poor prediction of the temperatures and the period of an exact model with defined inert zones while a boundary conditions based on long inert zones yield better results.

3.1.2. The detailed model

The fast nullcurve ($F(T_s, \theta^*) = 0$) and the slow nullcurve, $g(T_s, \theta^*) = 0$, are presented in Fig. 2 for increasing fluid temperatures of the detailed model. At relatively low gas temperatures the system has one stable low-activity steady state to which it converges. At about 478 K the system goes through a saddle-node bifurcation and two steady states appear on the unstable branch (Fig. 2b). All trajectories of the system now converges to the low-temperature steady state, and we refer to it as globally stable. As the gas temperature is further increased the two unstable steady states move in opposite directions on the unstable branch (Fig. 2c and d), until the saddle point coalesce with the steady node and disappear. From that point the system has one unstable steady state surrounded by a stable limit cycle to which the system converges (Fig. 2d). At a gas temperature of about 560 K the system goes through a Hopf bifurcation point where the unstable steady state passes the curve's turning point and becomes stable. At larger temperatures the system converges to the high-temperatures stable steady state.

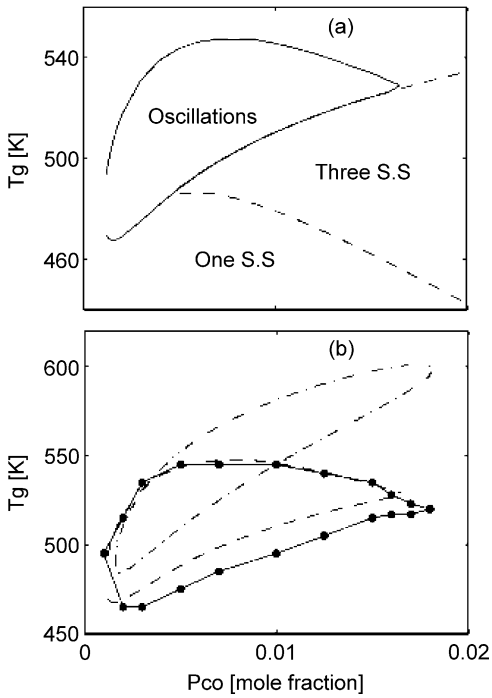

Fig. 3. (a) Bifurcation map of the catalyst particle (lumped system). (b) Comparison of the oscillatory domains of the kinetic model (-·-·-) of the catalyst particle (- - -) and of the reactor (solid line, the coordinates denote the temperature and concentration of the fee). $P_{O_2} = 0.21$ (after Keren and Sheintuch).

The bifurcation points were determined for various CO feed concentration, and the bifurcation map (Fig. 3a) shows a closed curve within which the system oscillates. There exists also a domain where the system acquires three steady states, of which only one is stable and the system converges to it. In the other areas of the parameter domain the system has one stable steady state. Thus, the system exhibits only two observable domains: a (globally or true) unique stable state and an oscillatory domain bounded by a Hopf bifurcation line on one side and a global-saddle-node along its boundary with cusp domain.

4. Simulated patterns

The discussion below classifies the emerging patterns for the homogeneous and heterogeneous models of an adiabatic reactor with exothermic positive-order oscillatory reactions, in terms of their phase planes. We later turn to the detailed model and show the commonality of behavior. The commonality stems from the symmetry-preserving interaction that exists in both reactors: An ignition upstream is transmitted quickly downstream inducing a similar process. We conclude this chapter by discussing several studies of isothermal reactor models, or of approximate solutions of nonadiabatic reactors, in which other patterns, due to symmetry-breaking interaction, may emerge.

The review below attempts to classify patterns in *homogeneous* and *heterogeneous* reactor models, and to demonstrate the effect of β and Pe_T numbers on the emerging patterns [2,16,17]. The results show that when $\beta_T > Pe_T$ the heterogeneous and the pseudo-homogeneous models show very similar patterns, but the results differ for other conditions:

- Almost homogeneous oscillations (periodic horizontal bands) emerge when the inlet is oscillatory: That is the case for low β_T (or low Pe_T numbers, when convection is accounted for) in Fig. 1a. In the corresponding patterns with $Pe_T \geq 100$ the fronts sweep the whole reactor (Fig. 4a). At large Pe_T it exhibits a stationary front that periodically sends narrow pulses downstream (Fig. 4b, $Pe_T = 10^4$). Recalculating the results with the homogeneous model yields surprisingly similar patterns (Fig. 4e and f).

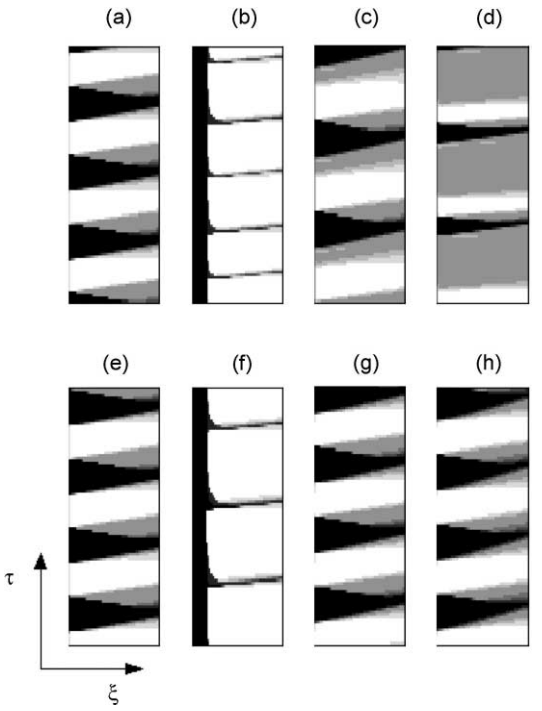

Fig. 4. Comparison between the heterogeneous (a–d) and the corresponding pseudo-homogeneous (e–h) model simulations for $\beta_T = 10^4$ (a and b), 10^2 (c) and 50 (d); Pe_T in (a–d) are 10^2 (a, c and d), 10^4 (b), while in (e–h) Pe_T and Pe_C follow Eqs. (14) and (15). $Da = 0.5$, $K = 1$, $M = 1.1$ (Fig. 1, line 1) (after [17]).

The difference between the two models become significant when $\beta_T < Pe_T$: Fig. 4 presents the simulations of the heterogeneous model with $Pe_T = 100$ and $\beta_T = 100$ (c) or 50 (d) (as opposed to $\beta_T = 10\,000$ in Fig. 4a and b) showing that the heterogeneous model is sensitive to the parameters while the pseudo-homogeneous one becomes insensitive to the effective *Pe* number. This, again, is predicted from the transformation (Eqs. (14) and (15)).

- The heterogeneous model exhibits a sharp front that oscillates around its stationary positions (Fig. 5b, $Pe_T = 3000$) when the sequence of phase planes is extinguished-bistable-ignited and the patterns are sustained over a relatively narrow domain of Pe_T numbers (the conditions corresponding to line 2, Fig. 1b, $\beta = 10^3$), With decreasing Pe_T the amplitude increases and at $Pe_T = 1000$ the front sweeps the whole surface. Again, when $\beta_T \gg Pe_T$ the corresponding solutions of the pseudo-homogeneous

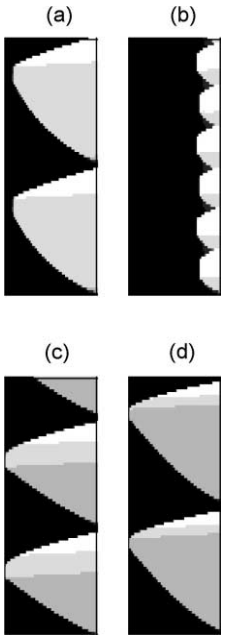

Fig. 5. Comparison of the heterogeneous (a,b) and corresponding pseudo-homogeneous model results (c,d) when Pe_T and β_T are comparable. $\beta = 10^3$; Pe_T are 1750 (a), 3000 (b), while in (c,d) Pe_T and Pe_C follow Eqs. (14) and (15); $Da = 0.06$, $K = 4$, $M = 2$ (Fig. 1, line 2) (after [17]).

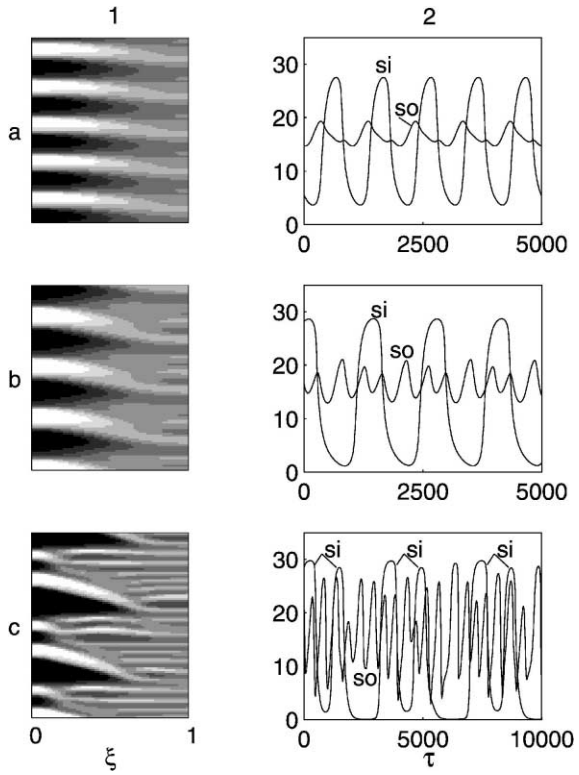

Fig. 6. Aperiodic patterns simulated by the heterogeneous model at low β_T (=1). $Da = 0.06$, $K = 0.1$, $M = 0.12$ (Fig. 1, line 3). Column 1 presents the spatiotemporal behavior of the solid temperature; column 2 the temporal behavior of the solid temperature at the inlet (si) or outlet (so). Pe_T are 20 (a), 50 (b), 500 (c) (after [17]).

model (not shown) show surprisingly similar results but the similarity breaks down when the two parameters are comparable and the corresponding solutions of the pseudo-homogeneous model are significantly different (Fig. 5c and d).

Significant differences between the two models occur for small β_T values, around unity. Fig. 6 presents the complex aperiodic behavior of the heterogeneous model with $\beta_T = \beta_C = 1$ showing simple periodic behavior with $Pe_T = 20$ (a), complex but periodic behavior with $Pe_T = 50$ (b) and apparently chaotic with $Pe_T = 500$. Similar aperiodicities were presented by [2]. The corresponding pseudo-homogeneous model exhibits an extinguished steady state, in all three cases, and is not shown.

- Upstream-moving pulses emerge when the inlet is oscillatory but the outlet is nonexcitable, as demonstrated in the previous example (Fig. 6a).
- Application of a local perturbation to the outlet or to the inlet of a bed lying in the excitable domain may induce a overshoot. When the bed is initially ignited the excitation will send a trigger front, that sweeps through the bed, followed by a relaxation back into the ignited state and a second trigger or phase front (Fig. 7).
- Split-band-patterns appear when new fronts are generated inside the reactor but they cannot propagate upstream due to refractory tail of the previous pulse. They form multiperiodic or aperiodic sequence of pulses. Successive coalescence of fronts, as they move upstream, may also generate an aperiodic pattern [2].

A typical spatiotemporal pattern of the catalyst temperature in a *detailed model* of CO oxidation along the converter is presented in Fig. 8. The hot front enters

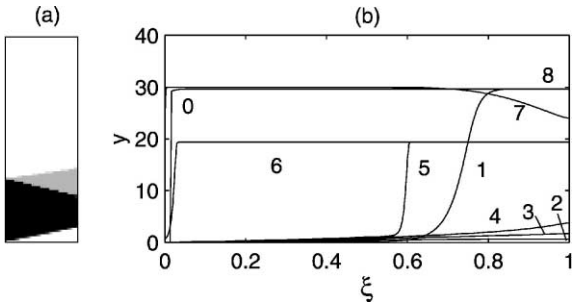

Fig. 7. The system response in an excitable state upon a perturbation at the inlet. In (b) 0 is an initially perturbed profile, 8 is a final steady-state profile, lines 0–8 are equally intervaled (after [16]).

the reactor from the outlet and advances to the reactor inlet. The hot domain disappears almost simultaneously all over the reactor length. The same behavior can be seen in Fig. 9, where the catalyst temperatures at the reactor feed, midpoint and exit are presented as a function of time. The oscillations are synchronized along the reactor and their amplitude decline along the reactor. Note again that ignition starts at the exit while extinction is simultaneous. The almost synchronous nature of the oscillations results from the strong convection term. Ignition of the reactor inlet will cause the fluid temperature to rise and the fluid concentration to decline downstream and these two effects will induce a transition downstream. Recall that the only unstable behavior in that problem is oscillatory motion and, as

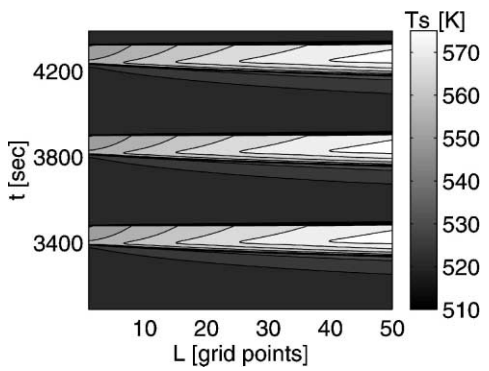

Fig. 8. A spatiotemporal pattern of the converter behavior presented as gray-scale contours ($P_{CO} = 0.01$, $P_{O_2} = 0.21$, $T_{in} = 510\,K$, $L = 1$ denote reactor inlet, $L = 50$ — reactor outlet) (after Keren and Sheintuch).

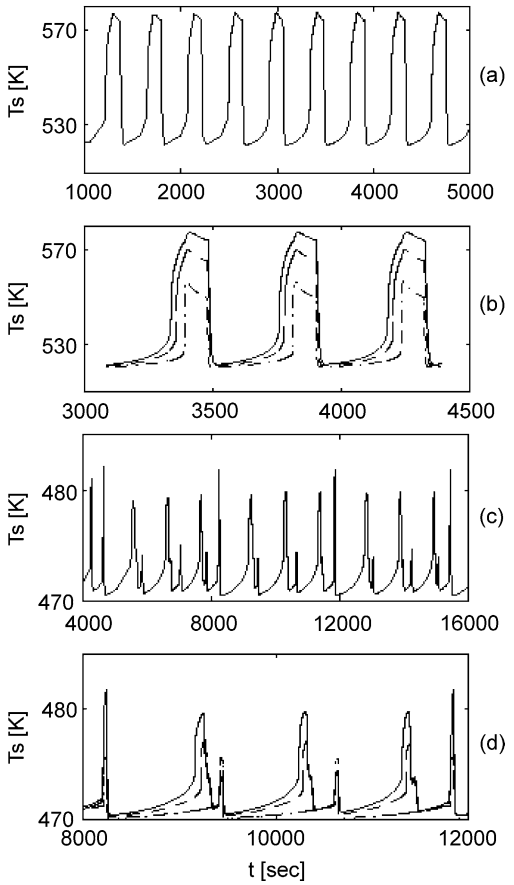

Fig. 9. Simple (a and b) and aperiodic (b and c) temporal oscillations of the reactor showing exit behavior for extended times (a and c) as well as detailed behavior (b and d) at the inlet (dash-dotted), middle (dashed) and outlet (solid line). ($C_{f_{in}}$, T_{in}) are (0.01, 510 K) in (a and b), and (0.002, 480) in (c and d). $P_{O_2} = 0.21$ (after Keren and Sheintuch).

expected, the behavior is quite similar to the generic first-order kinetics with oscillatory kinetics.

The oscillatory domain of the reactor was mapped and the oscillatory domain is compared in Fig. 3b with that of the isothermal kinetic model (i.e., with no resistance to heat and mass transfer) and with the oscillatory domain of the catalyst (lumped) problem. Due to the synchronous nature of the oscillations the lumped system still gives a good estimate of the oscillatory domain in the distributed system.

In some parts of the oscillatory domain the model exhibits a more complex behavior such as period-two oscillations (two peaks per period, not shown here) and

chaos (Fig. 9c and d). Fig. 9a and c show a long run of the catalyst temperature at the outlet while Fig. 9b and d present temperature distribution over few cycles. At a chaotic state the hot front enters irregularly the reactor outlet and moves toward the reactor inlet; as it moves inward it decays and does not reach the reactor inlet.

Since the detailed model presents a realistic accounts of a commercially important process we may attempt to use it to enhance performance. The bottleneck in improving the converter performance is the time required to reach high reactor temperatures when starting its operation with a cold engine (referred to as the cold start problem). One approach is to add resistive heating to the converter during that period. This problem will be beyond the scope of this work. Here we consider whether the operation of an extinguished reactor can be improved by applying thermal perturbation to the solid-phase. Such a perturbation will create a front that, with proper conditions, will travel through the system and ignite it. Subsequently the reactor will relax along the ignited state and eventually will extinguish, as does an excitable system. The activity along the extinguished state will slowly relax towards the initial steady state. After a sufficiently long period the perturbation may be applied again. The reactor will be ignited quickly after a perturbations at the inlet since the information will travel quickly downstream by fast convection (residence time is about 5×10^{-4} s). We simulated this approach to find that while a local perturbation can ignite the reactor quite quickly (within less than 10 s), relaxation is extremely slow, with the reactor reaching high-activities only after 2000 s. Thus, for most of the cycle the reactor is cold and inactive. Moreover, the reactor cannot be reignited until its activity is reestablished. Applying a periodic perturbation, of the type described above, will cause this cycle of events to repeat itself only if the perturbations are applied at sufficiently large intervals (Fig. 10).

Similar patterns may be realized in a one-dimensional model of an isothermal reactor with bistable or oscillatory kinetics. Shvartsman and Sheintuch [19–21] analyzed such a model, in which the local oscillator, similar to a reversible Brusselator, accounts for the reaction between two gas-phase species whose concentration vary along the reactor: species B (e.g. oxygen) is assumed to accelerate the rate while A

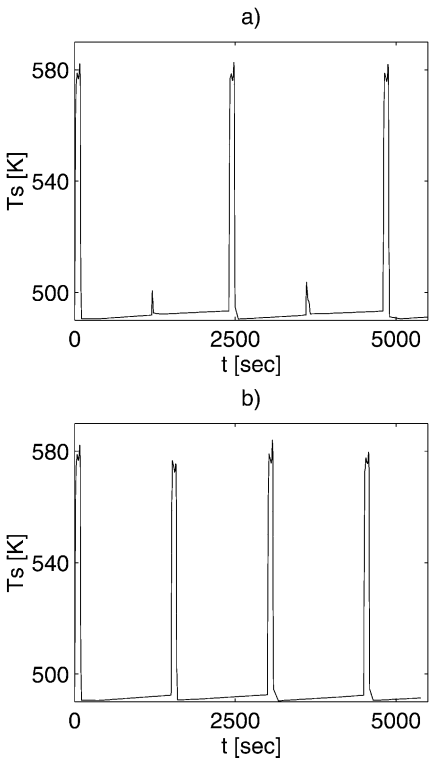

Fig. 10. Response of the reactor to periodic perturbations every 1200 s (a) or 1500 s (b) (after Keren and Sheintuch).

(e.g. CO) inhibits it; in the bistable domain the rate exhibits a clockwise hysteresis curve with varying C_A and a counterclockwise curve with varying C_B. Many of the patterns with A-limiting reactors were found to be very similar the thermal patterns in a nonisothermal reactor, described above, since both can be characterized by symmetry-preserving interaction. A PFR limited by B is characterized by symmetry-breaking interaction and may exhibit the following motions:

- Upstream- or downstream-moving pulses (parallel bands in the time–space diagram) or source points (V-shaped bands) emerge when the system spans the oscillatory domain; if the inlet or outlet are not excitable the pulses terminate short of the inlet or outlet, respectively.
- Stationary or oscillatory fronts emerge when the bistability domain is spanned; the amplitude of the front oscillations in the latter pattern may span the whole reactor.

5. Concluding remarks

Pattern formation have been analyzed for the homogeneous, heterogeneous and detailed models of a fixed catalytic adiabatic bed reactor with oscillatory kinetics. These three models account for one, two or three phases, respectively. The deeper phase (say adsorbed-phase) may respond quickly to conditions in the phase that wraps it or may exhibit bistability or oscillations with respect to conditions in the outer phase. In the former case we may lump the inner and outer phases. If the deeper phase exhibits local bistability its motion can be traced by a sequence of phase planes spanned by the reactor. Patterns observed with the three models were quite similar due to the similarity in phase planes and in the nature of interaction.

5.1. Observations

The number of experimental observations of such patterns is quite limited. Self-sustained dynamic behavior, in the form of successive birth and propagation of ignition and extinction fronts, was reported by [12] in a nonadiabatic reactor catalyzing CO oxidation. In the region of global monostability a hot spot emerged at the reactor inlet, propagated towards the outlet at an average velocity of 10^{-4} m/s, and died out as another hot spot was born at the inlet. A similar behavior was observed with the same reaction in an adiabatic fixed-bed [27]: A hot front emerged at the reactor inlet and moved downstream as its amplitude increase. Dvorak et al. [3] and Sheintuch and Adjaye [15] observed motions that can be interpreted as excitable waves motion (similar to Fig. 7) in response to a local perturbation at the inlet of an adiabatic reactor catalyzing C_2H_4 or CO oxidation, respectively. Setting a local perturbation at the inlet of a 30 cm long bed packed with Pt/Al_2O_3 catalytic pellets induced a front that moved at constant speed and shape, in the case of ethylene oxidation. The front always moved downstream until its exit. A hot spot appeared then at the inlet, it developed and spread across the reactor and the old steady state was established. In the case of CO oxidation local heating of the reactor inlet, or of an intermediate position, created an ignition front that propagated at constant speed through the bed followed by the extinction front.

The limited number of observations is due in part to experimental difficulties. This analysis suggests that patterns in an adiabatic reactor will be not as rich as in a cooled one, due to the symmetry-preserving nature of interaction. Conditions that induce symmetry-breaking interaction may emerge in a cooled isothermal-fluid reactor in which the fluid-temperature is constant but the solid-temperature varies. In that case an ignition at the inlet will induce declining concentrations downstream which will lead to extinction there. That was verified by an approximate solution that used piecewise linear kinetics [21]. These conditions, however, may be difficult to achieve experimentally.

Acknowledgements

Work supported by the Volkswagen-Stiftung Foundation. MS is a member of the Minerva Center of Nonlinear Dynamics and Complex Systems. ON is partially supported by the Center for Absorption in Science, Ministry of Immigrant Absorption State of Israel.

References

[1] V. Balakotaiah, Structural stability of nonlinear convection–reaction models, Chem. Eng. Educ. 30 (1996) 234–239.
[2] M. Barto, M. Sheintuch, Excitable waves and spatiotemporal patterns in a fixed-bed reactor, AlChe J. 40 (1994) 120–126.
[3] L. Dvorak, P. Pinkas, M. Marek, Dynamic behavior of CO catalytic afterburber with electric heating, Catal. Today 20 (1993) 449.
[4] G. Ertl, Oscillatory catalytic reaction at single-crystal surfaces, Adv. Catal. 37 (1990) 213–277.
[5] D.A. Frank-Kamenetskij, Diffusion and Heat Transfer in Chemical Kinetics, 2nd Edition, Plenum Press, New York, 1969.
[6] N. Hartmann, R. Imbihl, W. Vogel, Experimental evidence for an oxidation/reduction mechanism in rate oscillations of catalytic CO oxidation on Pt/SiO_2, Catal. Lett. 28 (1994) 373.
[7] V. Hlavacek, O. Van Rompay, Current problems of multiplicity, stability and sensitivity of states in chemically reacting systems, Chem. Eng. Sci. 36 (1981) 1587–1597.
[8] R. Imbihl, G. Ertl, Oscillatory kinetics in heterogeneous catalysis, Chem. Rev. 95 (1995) 697.
[9] I. Keren, M. Sheintuch, Modeling and analysis of spatiotemporal patterns in the catalytic converter with oscillatory kinetics, Chem. Eng. Sci. 55 (2000) 1461–1475.

[10] Z. Kurtanjek, M. Sheintuch, D. Luss, Surface state kinetic oscillations in the oxidation of hydrogen on nickel, J. Catal. 66 (1980) 11.
[11] T.H. Lindstrom, T.T. Tsotsis, Reaction rate oscillations during CO oxidation over $Pt/\gamma\text{-}Al_2O_3$; experimental observations and mechanistic causes, Surf. Sci. 150 (1985) 487.
[12] J. Puszynski, V. Hlavacek, Experimental study of ignition and extinction waves and oscillatory behaviour of a tubular nonadiabatic fixed bed reactor for the oxidation of carbon monoxide, Chem. Eng. Sci. 39 (1984) 681–692.
[13] B.C. Sales, J.E. Turner, M.B. Maple, Oscillatory oxidation of CO over Pt, Pd and Ir catalysts: theory, Surf. Sci. 114 (1982) 381–394.
[14] F. Schuth, X. Song, L.D. Schmidt, E. Wicke, Synchrony and the emergence of chaos in oscillations on supported catalysts, J. Chem. Phys. 92 (1990) 745–756.
[15] M. Sheintuch, J. Adjaye, Excitable waves in a fixed bed reactor: ethylene oxidation on platinum, Chem. Eng. Sci. 45 (1990) 1897.
[16] M. Sheintuch, O. Nekhamkina, Pattern formation in homogeneous reactor models, AIChE J. 45 (1999) 398–409.
[17] M. Sheintuch, O. Nekhamkina, Spatiotemporal patterns in homogeneous and heterogeneous models of catalytic reactors, Chem. Eng. Sci. 54 (1999) 4535–4546.
[18] M. Sheintuch, R.A. Schmitz, Kinetic modeling for oscillatory catalytic reactions, ACS Symp. Ser. 65 (1978) 488–497.
[19] M. Sheintuch, S. Shvartsman, Patterns due to convection–conduction–reaction interaction in a fixed-bed catalytic reactor, Chem. Eng. Sci. 49 (1994) 5315–5326.
[20] M. Sheintuch, S. Shvartsman, Spatiotemporal patterns in catalytic reactors, AIChE J. 42 (1996) 1041–1068.
[21] S. Shvartsman, M. Sheintuch, One- and two-dimensional spatiotemporal thermal patterns in a fixed-bed reactor, Chem. Eng. Sci. 50 (1995) 3125–3141.
[22] M.M. Slin'ko, N.I. Jaeger, Studies in Surface Science and Catalysis: Oscillating Heterogeneous Catalytic Systems, Vol. 86, Elsevier, Amsterdam, 1994, pp. 47–80.
[23] J.E. Turner, B.C. Sales, M.B. Maple, Oscillatory oxidation of CO over a Pt catalyst, Surf. Sci. 103 (1981) 54–74.
[24] C.G. Vayenas, B. Lee, J. Michaels, Kinetics, limit cycles, and mechanisms, of ethylene oxidation on platinum, J. Catal. 66 (1980) 36.
[25] D. Vortmeyer, R.J. Schaefer, Equivalence of one- and two-phase models for heat transfer processes in packed-beds: one-dimensional theory, Chem. Eng. Sci. 29 (1974) 485.
[26] W. Wicke, D. Vortmeyer, Zudzonen heterogener reaktionen in gasdurchstromten kornerschichten, Z. Elektochem. Ber. Bunsenges. Phys. Chem. 63 (1959) 145–152.
[27] E. Wicke, H.U. Onken, Periodicity and chaos in a catalytic packed bed reactor for CO oxidation, Chem. Eng. Sci. 43 (1988) 2289–2904.